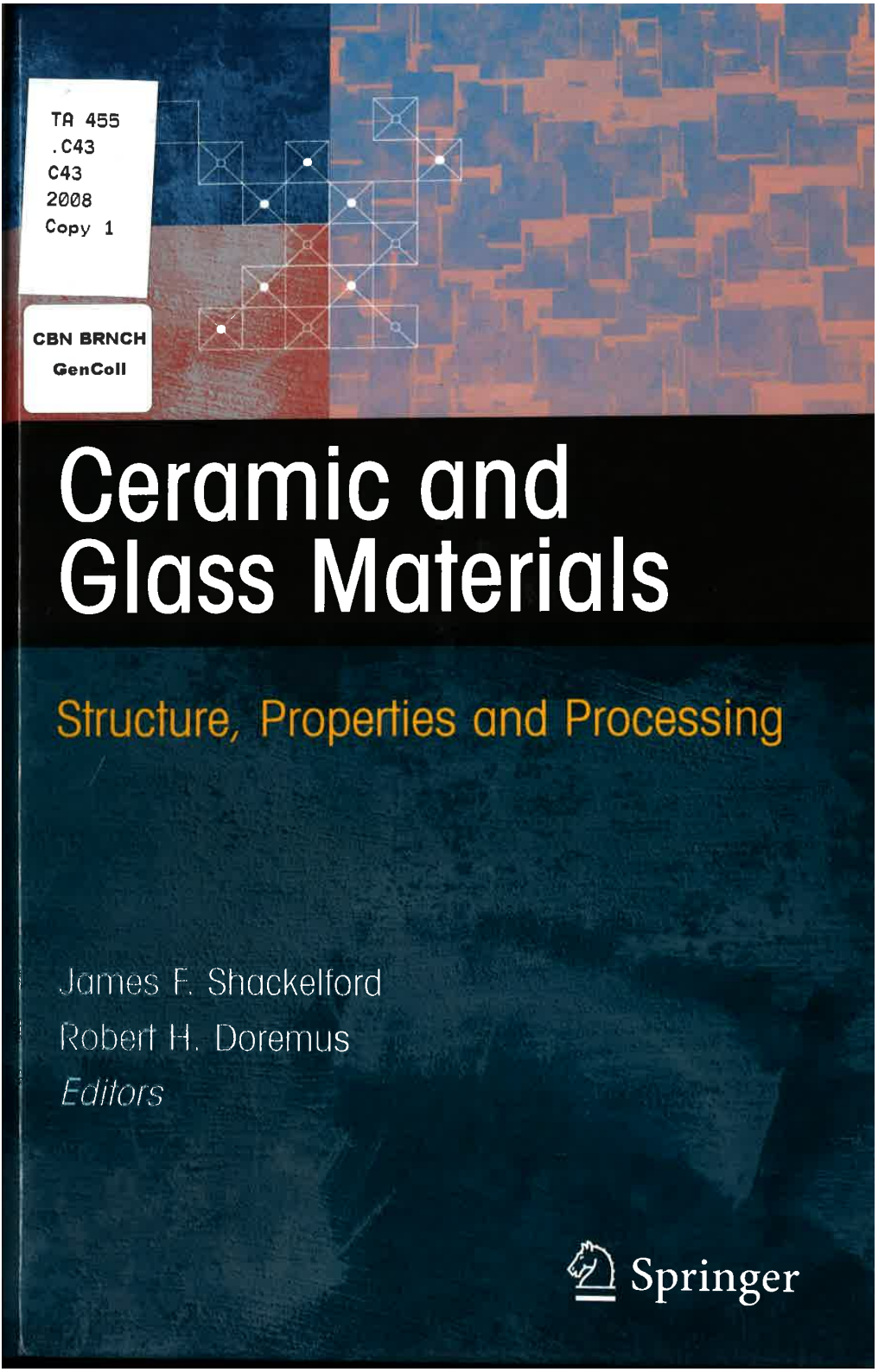


Masimo Ex. 1042
IPR Petition - USP 10,627,783

James F. Shackelford • Robert H. Doremus
Editors

Ceramic and Glass Materials

Structure, Properties and Processing

Springer

Masimo Ex. 1042
IPR Petition - USP 10,627,783

Editors
James F. Shackelford
University of California, Davis
Dept. Chemical Engineering
& Materials Science
1 Shields Avenue
Davis, CA 95616

Robert H. Doremus
Materials Research Center
Rensselaer Polytechnic Institute
Dept. Materials Science & Engineering
110 8th Street
Troy, NY 12180-3590

ISBN 978-0-387-73361-6 e-ISBN 978-0-387-73362-3
DOI 10.1007/978-0-387-73362-3

Library of Congress Control Number: 2007938894

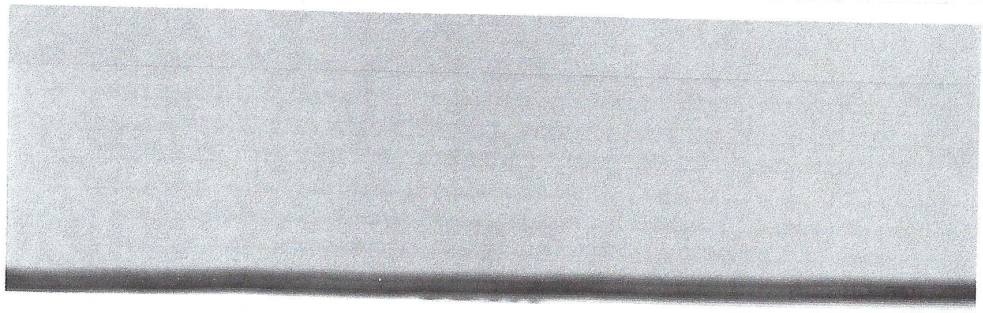
© 2008 Springer Science+Business Media, LLC
All rights reserved. This work may not be translated or copied in whole or in part without the written permission of the publisher (Springer Science+Business Media, LLC, 233 Spring Street, New York, NY 10013, USA), except for brief excerpts in connection with reviews or scholarly analysis. Use in connection with any form of information storage and retrieval, electronic adaptation, computer software, or by similar or dissimilar methodology now known or hereafter developed is forbidden.
The use in this publication of trade names, trademarks, service marks, and similar terms, even if they are not identified as such, is not to be taken as an expression of opinion as to whether or not they are subject to proprietary rights.

Printed on acid-free paper

9 8 7 6 5 4 3 2 1

springer.com

Masimo Ex. 1042
IPR Petition - USP 10,627,783



Robert H. Doremus – A Dedication

With sadness, I note that in late January 2008 while finishing the editing of this book, Bob Doremus passed away suddenly in Florida. His wife and one of his daughters were with him at the time. Characteristic of his meticulous attention to detail, he had just finished personally preparing the index for this volume. Professor Doremus was an icon of ceramic and glass science, and this volume is a fitting tribute to his career. In addition to editing the book, he provided the opening chapter on alumina, the quintessential structural ceramic material.

After finishing *two* Ph.D. degrees in physical chemistry (University of Illinois, 1953 and University of Cambridge, 1956), Dr. Doremus worked at the General Electric Research and Development Laboratory for many years during a period of time that can fairly be described as a "golden age" of ceramic and glass science. His colleagues included Robert Coble, Joseph Burke, and Paul Jorgensen. There, he conducted seminal research including classic studies of gas and water diffusion in ceramics and glasses.

In 1971, he moved to the Department of Materials Science and Engineering at the Rensselaer Polytechnic Institute and began a long career as an educator. He continued to work on a broad range of topics in ceramic and glass science and was especially well known for publishing the definitive version of the important alumina-silica phase diagram [Klug, Prochazka, and Doremus, *J.Am.Ceram.Soc.*, **70** 750 (1987)] as well as doing pioneering work on bioceramics for medical applications. At Rensselaer, Bob was named the New York State Science and Technology Foundation Professor of Glass and Ceramics and served as Department Chair from 1986 to 1995.

Appropriate to his distinguished career as a scientist and educator, Bob received numerous awards in recognition of his accomplishments. Resulting in nearly 300 publications, his research contributions were recognized with the Scholes Award of Alfred University, the Morey Award of the American Ceramic Society, and the Ross Coffin Purdy Award, the American Ceramic Society's top honor for research. He received numerous teaching awards while at Rensselaer, including the Outstanding Educator Award of the American Ceramic Society. His winning the top research *and* educator awards of the American Ceramic Society is symbolic of his remarkable career.

Beyond these professional accomplishments of a great scientist and dedicated teacher, Bob Doremus was a devoted family man and leaves behind his wife Germaine

Masimo Ex. 1042
IPR Petition - USP 10,627,783

and children Carol, Elaine, Mark, and Natalie. As with his family, Bob cared deeply about his students and worked tirelessly to help them. He was also a fine and supportive colleague. He will be greatly missed, and this book is dedicated to him with both affection and respect.

J.F. Shackelford
Davis, CA
February 2008

Masimo Ex. 1042
IPR Petition - USP 10,627,783

This material may be protected by Copyright law (Title 17 U.S. Code)

Contents

Preface vii

Contributors xi

Chapter 1 **Alumina** 1
Robert H. Doremus

Chapter 2 **Mullite** 27
David J. Duval, Subhash H. Risbud, and James F. Shackelford

Chapter 3 **The Sillimanite Minerals: Andalusite, Kyanite, and Sillimanite** 41
Richard C. Bradt

Chapter 4 **Aluminates** 49
Martin C. Wilding

Chapter 5 **Quartz and Silicas** 71
Lilian P. Davila, Subhash H. Risbud, and James F. Shackelford

Chapter 6 **Refractory Oxides** 87
Jeffrey D. Smith and William G. Fahrenholtz

Chapter 7 **Clays** 111
William G. Fahrenholtz

Chapter 8 **Concrete and Cement** 135
Mariano Velez

Chapter 9 **Lead Compounds** 151
Julie M. Schoenung

Masimo Ex. 1042
IPR Petition - USP 10,627,783

Chapter 10 **Zirconia** **169**
Olivia A. Graeve

Index **199**

Masimo Ex. 1042
IPR Petition - USP 10,627,783

Chapter 1
Alumina

Robert H. Doremus

The uses, processing, structure, and properties of alumina are summarized in this article. Various polymorphs of alumina and its phase relations with other oxides are described. The following properties are discussed: mechanical, thermal, thermodynamic, electrical, diffusional, chemical, and optical. Quantitative values for these properties are given in tables. The usefulness of alumina results from its high strength, melting temperature, abrasion resistance, optical transparency, and electrical resistivity. Traditional uses of alumina because of these properties are furnace components, cutting tools, bearings, and gem stones; more recent applications include catalyst substrates, tubes for arc lamps, and laser hosts. Possible new uses of alumina are in electronic circuits, optical components, and biomaterials. Alumina fibers for composites and optics must be pure, defect free, and cheap.

1 Introduction

Alumina (Al_2O_3) is one of the most important ceramic materials, both pure and as a ceramic and glass component. Some uses of alumina are given in Table 1; an exhaustive and detailed description of many of these uses is given in [1]. There are also extensive discussions of uses of alumina in [2]. Processing of alumina is discussed in both these references, and [2] has a summary of some properties of alumina. In writing this review, I have relied on material from these references. Anyone interested in more details of processing and properties of alumina should obtain [2] from the American Ceramic Society. Reference [1] is also available from the Society and has additional information on processing and uses of alumina. More recently, there have been two issues of the Journal of the American Ceramic Society devoted to alumina [3, 4]; these issues concentrate on defects and interfaces, especially grain boundaries [3], grain growth, and diffusion in alumina [4].

The usefulness of alumina derives from a variety of its properties. It has a high melting temperature of 2,054°C, and is chemically very stable and unreactive, leading to applications as high-temperature components, catalyst substrates, and biomedical implants. The hardness, strength, and abrasion resistance of alumina are among the highest for oxides, making it useful for abrasive materials, bearings,

J.F. Shackelford and R.H. Doremus (eds.), *Ceramic and Glass Materials: Structure, Properties and Processing*.
© Springer 2008

Masimo Ex. 1042
IPR Petition - USP 10,627,783

Table 1 Uses of Alumina

Solid alumina
Furnace components
Catalyst substrates
Electronics substrates
Electrical insulators
Cutting tools
Bearings
Spark Plugs
Arc lamp tubes
Laser hosts
Gem stones
Alumina powders
Abrasives
Catalyst pellets
Alumina coatings
Oxidation protection of aluminum and aluminum alloys
Capacitors
Transisitors
Bioceramics
Alumina fibers
Thermal insulators
Fire retardation
Alumina as a component of
Ceramics and glasses
Mullite components
Electrical insulators
Porcelains
Durable glasses

and cutting tools. The electrical resistance of alumina is high, so it is used pure and as a component in electrical insulators and components. Alumina has excellent optical transparency, and along with additives such as chromium and titanium, it is important as a gem stone (sapphires and rubies) and a laser host (ruby). Because of its high melting temperature, chemical inertness, and optical transparency, it is highly useful for containing arcs in street lamps. See Table 1 and also [1, 2] for more on uses of alumina.

In this review, the processing of alumina is discussed next, and then its properties are tabulated and described. In a summary future uses of alumina are considered.

2 Processing

2.1 *Raw Materials*

Bauxite is the name of the ore that is the primary source of alumina; bauxite contains gibbsite, γ-$Al(OH)_3$, which is the stable phase of $Al(OH)_3$ at ambient temperature and pressure. The structure of alumina and hydrated alumina phases are listed in Table 2.

Masimo Ex. 1042
IPR Petition - USP 10,627,783

Table 2 Structures of stable alumina (corundum) and unstable aluminas

Designation	Structure	Lattice Parameters, angle (Å)		
		a	*b*	*c*
Corundum	Hexagonal (rhombohedral)	4.758		12.991
Eta	Cubic (spinel)	7.90		
Gamma	Tetragonal	7.95		7.79
Delta	Tetragonal	7.97		23.47
Theta	Monoclinic	5.63	2.95	11.86 103° 42′
Kappa	Orthorhombic	8.49	12.73	13.39

Bauxite from the Guianas in South America is low in iron and silica impurities, so it is preferred when purity is important. Other important sources of bauxite are in Brazil, the southern United States, Southeast Asia, West Africa, and India.

2.2 *Processing*

Aluminum hydroxides are separated from bauxite by the Bayer process, in which these hydroxides are dissolved in sodium hydroxide to separate them from the other unwanted constituents of the bauxite. The dissolution reactions are carried out at about 285°C and 200 atm. pressure, and are:

$$Al(OH)_3(s) + NaOH(soln) = NaAl(OH)_4(soln) \quad (1)$$

$$AlOOH(s) + H_2O(soln) + NaOH(soln) = NaAl(OH)_4(soln) \quad (2)$$

in which (s) stands for solid and (soln) for solution. The solution containing $NaAl(OH)_4$ is separated from the unwanted solid impurities by sedimentation and filtration, and the solute is cooled to about 55°C. The aluminum hydroxides precipitate from the solution, aided by the addition of gibbsite seeds. The dried precipitated alumina or aluminum hydroxides can be used directly or further purified by resolution and reprecipitation. Other methods for preparing alumina and aluminum hydroxides from bauxite are described in [1, 2].

The stable phase of alumina at all temperatures and ambient pressure (one atm, or (1.01) 10^5 Pa) is corundum or α-Al_2O_3 (see Table 2). In single-crystal form, corundum is called sapphire. No phase transformation of corundum up to 175 GPa pressure has been observed experimentally [5, 6]; however, a calculation predicts that corundum should transform to the Rh_2O_3 (II) structure at about 78 GPa, and to a cubic perovskite structure at 223 GPa [7]. The Rh_2O_3 (II) structure has an X-ray pattern close to the corundum structure, so the transformation may have been missed in experimental studies.

Solid polycrystalline alumina is made from alumina powder by sintering. The traditional sintering methods for ceramics involve forming a powder into "green" ware, partially drying it at low temperatures, possibly "calcining" (heating) it at intermediate temperatures (perhaps 900°–1,100°C), and firing it to a dense solid at high temperature, for alumina above 1,400°C.

Masimo Ex. 1042
IPR Petition - USP 10,627,783

The time and temperature required to form the desired degree of porosity in the dense solid depend mainly on the particle size of the alumina powder. The usual sintering sequence is imagined to be: (1) neck formation between powder particles, (2) formation of open porosity with a continuous solid phase (intermediate stage), and (3) removal of closed pores imbedded in the dense solid. In the usual practical sintering of alumina, stage one is rapid, and the final density or porosity is determined mainly by stage three.

Various other oxides have been added to alumina to reduce the porosity of the final sintered solid. An especially valuable finding by Coble [9] was to add MgO to pure alumina powder; the resulting sintered alumina can be translucent (partial transmission of light). Usually sintered ceramics are opaque because of light scattering from residual pores, but in the translucent alumina, called Lucalox™, the porosity is low enough to reduce this scattering, so that Lucalox tubes are used in street lamps for containing a sodium arc. Because the lamp can be operated at high temperature, it is quite efficient.

Dense alumina can also be made by melting, but the high-melting temperature of 2,054°C makes this process expensive and difficult to control. High-value materials such as gem stones and laser hosts can be made by adding various colorants such as chromium, titanium, iron, cobalt, and vanadium to the melt.

In the sintering of alumina powders, the desired shape is formed in the green state before drying and firing. Various other constituents can be added to the starting powder. The density of the final product can be increased by hot-pressing, that is, by carrying out the firing under pressure. This method is expensive, so it is used only for high value polycrystalline products.

Alumina refractories for use in high temperature applications such as glass melting furnaces are usually made by the fusion-cast process. Various other oxides, such as SiO_2, MgO, Cr_2O_3, and ZrO_2 are added to the alumina powder to lower its melting point, and the resulting mixture is melted in an electric furnace and cast into the desired shapes for refractory applications. See the section on phase diagrams for the melting temperatures and compositions of a few mixtures of alumina with other oxides.

3 Structures of Pure and Hydrated Alumina

The structures of aluminas and hydrated aluminas are given in Tables 2 and 3. The only stable phase of Al_2O_3 is corundum at all temperatures and up to at least 78 GPa pressure (see earlier discussion). The corundum structure is shown in Fig. 1. It consists of oxygen ions in a slightly distorted close-packed hexagonal (rhombohedral) lattice, space group R3c. The aluminum ions occupy two-thirds of the octahedral sites in the oxygen lattice. The lattice parameters for corundum in Table 2 are for a hexagonal unit cell containing 12 Al_2O_3 molecules. The rhombohedral lattice parameters are a = 5.128 Å and $\alpha = 55.28°$. The ionic porosity Z of a solid is given by the formula

$$Z = 1 - V_a/V \tag{3}$$

in which V_a is the volume of atoms in a molecule (or in the unit cell) and V is the specific volume, or the volume of the unit cell. For alumina $Z = 0.21$ with the radius

Masimo Ex. 1042
IPR Petition - USP 10,627,783

Table 3 Structures of hydrated alumina phases

Phase	Formula	Lattice parameters (Å)/angle		
		A	*B*	*c*
Bayerite β-$Al(OH)_3$	Monoclinic	4.72	8.68	5.06/90°7′
Gibbsite α-$Al(OH)_3$	Monoclinic	8.64	5.07	9.72/85°26′
Boehmite α-AlOOH	Orthorhombic	2.87	12.23	3.70
Diaspore β-AlOOH	Orthorhombic	4.40	9.43	2.84

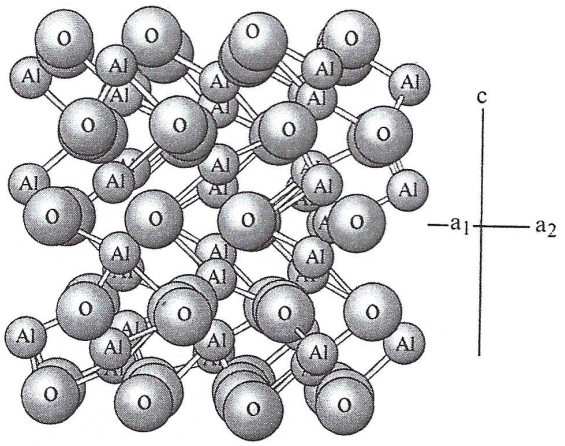


Fig. 1 The structure of alpha alumina from [31]. The structure of corundum (alpha-alumina) from [31]. The aluminum atoms occupy two-thirds of the octahedral interstices in a hexagonal close-packed array of oxygen atoms, which is distorted because the octahedral share faces in pairs

of 1.38 Å for oxygen atoms, so the structure has less "open" volume even than close-packing ($Z = 0.26$) of uniform spheres.

The various metastable alumina structures are all less dense than corundum. Several other allotropic structures have been suggested, but are less well-verified than those in Table 2. All these metastable aluminas have oxygen packings that are near to close-packed cubic. Usually, eta or gamma aluminas are formed at low temperatures, and transform in the sequence gamma→delta→theta→alpha alumina with increasing temperatures. However, many other variants are possible, with gamma formed at higher temperatures and transforming directly to alpha. See [8] for some previous references. Factors such as particle size, heating rate, impurities, and atmosphere can influence the kinetics of transformation and the sequence of phases. Above about 1,200°C, only alpha phase (corundum) is usually present.

The structures of various hydrated aluminas are given in Table 3. One configuration suggested for these structures is chains of Al–O bonds with hydrogen bonding between chains. These hydrated aluminas decompose at low temperature (about 300°C) to Al_2O_3 and water.

Masimo Ex. 1042
IPR Petition - USP 10,627,783

4 Equilibrium Binary Phase Diagrams of Alumina with Other Oxides

The most important binary oxide and ceramic phase diagram is the alumina–silica (Al_2O_3–SiO_2) diagram, shown in Fig. 2, as determined by Klug [10]. Important features in this diagram are the very low solid solubility of SiO_2 in Al_2O_3 and Al_2O_3 in SiO_2 and the single stable intermediate solid phase of mullite, which has the composition $3Al_2O_3$–$2SiO_2$; at higher temperatures, the amount of alumina in mullite increases. In contrast to binary metal systems, which usually have considerable solid solubility in the pure components and limited solubility in intermetallic phases, there is some solid solubility in mullite and very little in the end members of SiO_2 (cristobalite) and Al_2O_3 (corundum).

There is complete solid solubility in the system Al_2O_3–Cr_2O_3; both end members have the corundum structure [11, 12]. There is also subsolidus phase separation in this system [13]. There is also considerable solid solubility in the end-member oxides in the Al_2O_3–Fe_2O_3, Al_2O_3–Y_2O_3, and Al_2O_3–Ga_2O_3 systems [12]. Thus, the solid solubility results because the three-valent ions of Cr, Fe, Y, and Ga can substitute for aluminum in the corundum structure, and aluminum substitutes for these ions in their oxides. Alternatively, the solubilities of oxides with cation valences other than plus three are usually very low. For example, the solubility of magnesia in alumina is about 1 ppm atom fraction (Mg/Al) at 1,200°C [14]. Thus in mixtures of Al_2O_3 with higher concentrations of MgO than 1 ppm, second phases containing MgO can form on grain boundaries at 1,200°C and lower temperatures, but the Mg atoms do not dissolve or substitute for Al in the Al_2O_3. In the literature, there are many reports of higher solubilities of ions with valences different from three in

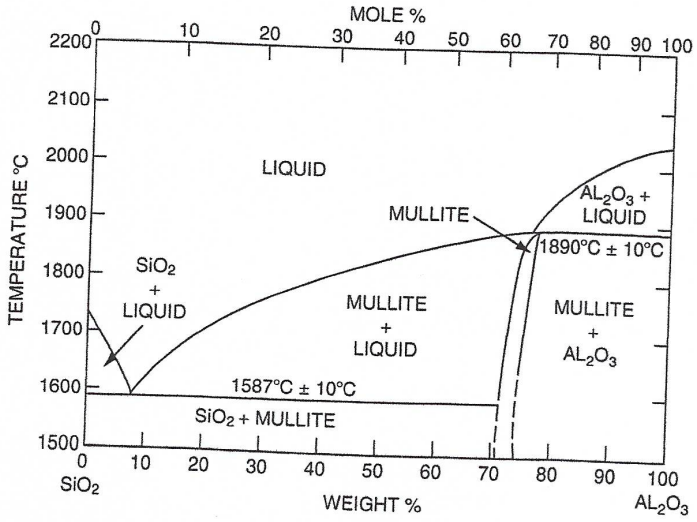


Fig. 2 The alumina–silica phase diagram. From [10]

Masimo Ex. 1042
IPR Petition - USP 10,627,783

alumina, but in view of the very careful work of Greskovitch and Brewer [14] with extremely pure alumina, these higher solubilities are unlikely.

In [1] there is a table (XI, on page 63) of minimum melting temperatures for a variety of binary alumina-oxide systems. With most oxides, these eutectic or peritectic temperatures vary from about 1,500 to 2,000°C. The Al_2O_3–V_2O_5 system has an anomalously low eutectic of 660°C at 99% V_2O_5; other low melting mixtures are Al_2O_3–Bi_2O_3 of 1,070°C, Al_2O_3–WO_3 of 1,230°C, and Al_2O_3–B_2O_3 of 1,440°C.

5 Mechanical Properties

5.1 Elasticity

Alumina shows the deformation behavior of a typical brittle solid, which is linear elasticity to failure. Elastic deformation is instantaneous when stress is applied, and is completely reversible when it is removed. In a tensile test of a rod or bar of alumina, the strain is linear with stress to failure; the slope of this stress–strain curve is the Young's modulus. Values of various moduli and Poisson's ratio for pure, dense polycrystalline alumina are given in Table 4 (from [15]). These values are considerably higher than those for most other oxides, as a result of the strong (high energy) aluminum–oxygen bonds in alumina. The various elastic constants of single crystal alumina are given in Table 5. As the temperature increases the elastic moduli decrease (as shown in Table 6) because of the increase in atomic displacements as the temperature increases, and consequent reduced bond strength.

Table 4 Elastic properties of polycrystalline alumina at room temperature [15], moduli in GPa

Young's modulus	403
Shear modulus	163
Bulk modulus	254
Poisson's ratio	0.23

Table 5 Elastic properties of single crystal alumina at room temperature [2, 15] in GPa

C11	498	S11	23.5
C12	163	S12	7.2
C13	117	S13	3.6
C14	–23.5	S14	4.9
C33	502	S33	21.7
C44	147	S44	69.4

Table 6 Temperature dependence of Young's modulus for polycrystalline alumina [2]

Temp. (°C)	Young's modulus (GPa)
25	403
500	389
1,000	373
1,200	364

Masimo Ex. 1042
IPR Petition - USP 10,627,783

5.2 Strength

The mechanical strength of a brittle material such as alumina depends on fl (cracks) in the alumina surface. When a tensile stress is applied perpendicular t deep, thin crack, the stress at the tip of the crack is greatly magnified above applied stress. Thus, the surface condition of a brittle solid determines it streng Surface flaws develop from abrasion, so the higher the abrasion resistance of a bri solid the greater its practical strength. Strengths of alumina are given in Table 7.

If a solid has no surface or internal flaws (a "perfect" lattice), it should have v high strength. Various theoretical equations for this ultimate strength S of a bri solid have been proposed; one is [16]

$$S^2 = E\gamma/4b \qquad (4$$

in which E is Young's modulus, γ is the surface energy, and b the lattice parame With $E = 403$ GPa (Table 4), $\gamma = 6.0$ J m^{-2} [17, 18], and $b = 0.177$ nm, the ultim strength S of alumina is about 58 GPa. This value is very high because of the hi bond strength of alumina; for example, silicate glasses and quartz have theoreti strength values of 18 GPa or lower.

Practical strengths of brittle materials vary over wide ranges depending on th surface condition and history. For alumina, tensile or bonding strengths vary ove wide range of values because of different surface conditions, resulting in differ flaw depths and flaw distributions. See [19] for a discussion of flaw distributi functions. The strength values for alumina are higher than for most other oxides; course all of these strengths are far smaller than the theoretical strength, and depe strongly on the history and treatment of the samples. As the temperature increas the strength of alumina decreases (as shown in Table 7) because of the increase atomic vibrations and reduction in bond strength, just as for the reduction in elas modulus with temperature. The strength of polycrystalline alumina depends strong on its grain size, as shown by one set of strength values from [2]. See also [20] f strengths of alumina machined and annealed at different temperatures. The streng also decreases as the alumina becomes more porous, as shown in Table 8; isolat pores increase the applied stress on their surfaces, and open porosity means mu more surface for flaw development.

Table 7 Bend strengths of alumina in MPa

Theoretical strength 58,000 at 25°C				Ref.
Single crystals (sapphire) 300–700 at 25°C				2
Polycrystals with similar treatment, as a function of grain size in micrometers:				2
Grain size →	1–2	10–15	40–50	2
Temp (°C)				
25°C	460	330	240	
400°C	360	260	230	
1,000°C	340	260	210	
1,350°C	260	110	97	

Masimo Ex. 1042
IPR Petition - USP 10,627,783

Table 8 Effect of porosity on the bend strength of polycrystalline alumina at 25°C from [2]

Porosity (%)	Strength (MPa)
0	269
10	172
20	110
30	76
40	55
50	47

5.3 *Fatigue*

The strengths of crystalline and glassy oxides decrease with time under a constant applied load. This static fatigue is usually modeled with a power law equation between times to failure t when a sample is subjected to an applied stress s:

$$\log t = c - n \log s \tag{5}$$

in which c is a constant and the stress exponent n is a measure of the susceptibility of the material to fatigue. The larger the n value the more resistant the material is to fatigue. Typical values of n for silicate glasses are 13 or lower [21]; for alumina an n value of about 35 was found [21], showing that alumina has much better fatigue resistance than most other oxides under ambient conditions.

This fatigue in oxides results from reaction with water, which can break the cation–oxygen bonds in the material; for example in alumina:

$$Al - O - Al + H_2O = AlOH + HOAl \tag{6}$$

Thus, when the ambient atmosphere is dry the fatigue failure time is long, and as the humidity increases the fatigue time decreases.

5.4 *Hardness*

The hardness of a material is measured by pressing a rod tip into a material and finding the amount of deformation from the dimensions of the resulting indentation. Hardness measurements are easy to make but hard to interpret. The stress distribution under the indenter is complex, and cracking, elastic and anelastic deformation, faulting, and plastic deformation are all possible around the indentation. Alumina is one of the hardest oxides. On the nonlinear Mohs scale of one to ten, alumina is nine and diamond is ten, but diamond is about a factor of three harder than alumina. Some approximate Knoop hardness (elongated pyramidal diamond indenter) values for alumina are given as a function of temperature in Table 9, and in Table 10 for some hard ceramics [22, 23]. It is curious that the hardness of alumina decreases much more than the strength as the temperature is increased.

Masimo Ex. 1042
IPR Petition - USP 10,627,783

Table 9 Knoop hardness of alumina as a function of temperature

T (K)	Hardness (kg mm^{-2})
400	1,950
600	1,510
800	1,120
1,000	680
1,200	430
1,400	260
1,600	160

Table 10 Knoop hardness values of some ceramics at 25°C from [2, 22]

Material	Hardness (kg mm^{-2})
Diamond	8,500
Alumina	3,000
Boron carbide	2,760
Silicon carbide	2,480
Topaz ($Al_{12}Si_6F_{10}O_{25}$)	1,340
Quartz (SiO_2)	820

5.5 *Creep*

Creep is the high-temperature deformation of a material as a function of time. Oth high-temperature properties related to creep are stress and modulus relaxation, inte nal friction, and grain boundary relaxation. The creep rate increases strongly wit temperature, and is often proportional to the applied stress. Microstructure (grai size and porosity) influences the creep rate; other influences are lattice defect stoichiometry, and environment. Thus, creep rates are strongly dependent on sampl history and the specific experimental method used to measure them, so the onl meaningful quantitative comparison of creep rates can be made for samples with th same histories and measurement method. Some torsional creep rates of differer oxides are given in Table 11 to show the wide variability of creep values. Compare with some other high temperature materials such as mullite ($3Al_2O_3 \cdot 2SiO_2$), alumin has a higher creep rate, which sometimes limits its application at high temperature (above about 1,500°C). See [24] for a review of creep in ceramics and [25] for review of creep in ceramic–matrix composites.

5.6 *Plastic Deformation*

At high temperatures (above about 1,200°C) alumina can deform by dislocatio motion. The important paper by Merritt Kronberg [26], see also [1], p. 32, an [27], showed the details of dislocation motion in alumina. Basal slip on the close packed oxygen planes is most common in alumina, with additional slip system on prism planes.

Masimo Ex. 1042
IPR Petition - USP 10,627,783

Table 11 Torsional creep rates of some polycrystalline oxides at 1,300°C and 124 MPa applied stress (from [23], p. 755)

Material	Creep rate ($\times 10^5\,h^{-1}$)
Al_2O_3	0.13
BeO	30
MgO (slip cast)	33
MgO (pressed)	3.3
$MgAl_2O_4$, spinel (2–5 μm grains)	26
$MgAl_2O_4$ (1–3 μm grains)	0.1
ThO_2	100
ZrO_2	3

5.7 *Fracture Toughness*

The fracture toughness K_{IC} of a brittle material is defined as

$$K_{IC} = YS\sqrt{c} \tag{7}$$

in which S is the applied stress required to propagate a crack of depth c, and Y is a geometrical parameter. Values of K_{IC} are often measured for ceramics from the lengths of cracks around a hardness indent. K_{IC} is not material parameter; it depends on sample history and many uncontrolled factors. It is based on the Griffith equation, which gives a necessary but not sufficient criterion for crack propagation [18]. Thus K_{IC} is not a very useful quantity for defining mechanical properties of brittle material. A value of about 3.0 $MPam^{1/2}$ is often found for alumina [1].

6 Thermal and Thermodynamic Properties

6.1 *Density and Thermal Expansion*

The density of alpha alumina at 25°C is 3.96 g cm^{-3}, which gives a specific volume of 25.8 $cm^3\,mol^{-1}$ or 0.0438 nm^3 per Al_2O_3 molecule. Densities of other aluminas are given in Table 12.

The coefficient of thermal expansion α of alumina at different temperatures is given in Table 13. Often an average value of α is given over a range of temperatures, but the slope of a length vs. temperature plot at different temperatures is a more accurate way of describing α.

6.2 *Heat Capacity (Specific Heat) and Thermodynamic Quantities*

The specific heat, entropy, heat and Gibbs free energies of formation of alumina are given in Table 14, from [28]. Above 2,790°K, the boiling point of aluminum, there is a discontinuous change in the heat of formation of alumina.

Masimo Ex. 1042
IPR Petition - USP 10,627,783

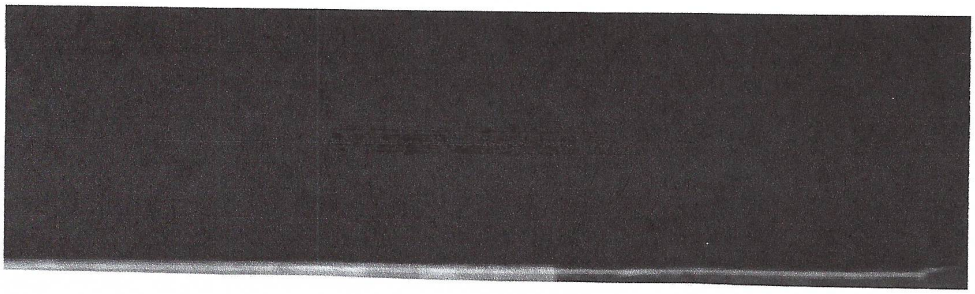


Table 12 Densities of anhydrous and hydrated aluminas

Material	Density (g cm^{-2})
Sapphire (α-$A_{l_2}O_3$)	3.96
γ-Al_2O_3	3.2
δ-Al_2O_3	3.2
κ-Al_2O_3	3.3
θ-$A_{l_2}O_3$	3.56
$Al(OH)_3$ gibbsite	2.42
AlOOH diaspore	3.44
AlOOH boehmite	3.01

From [1]

Table 13 The coefficient of linear thermal expansion of α–alumina as a function of temperature

Temp. (°C)	$d\alpha/dT$ ($\times 10^6$ per °C)
1,000	12.0
800	11.6
600	11.1
400	10.4
200	9.1
100	7.7
50	6.5

From [23]

Table 14 Specific heat and thermodynamic properties of α-alumina as a function of temperature

	Specific heat	Entropy	Heat of formation	Free energy of formation
T (K)	J mol^{-1} K^{-1}		kJ mol^{-1}	
0	0	0	−1663.608	−1663.608
100	12.855	4.295	−1668.606	−1641.692
200	51.120	24.880	−1673.388	−1612.636
298.15	79.015	50.950	−1675.692	−1582.275
400	96.086	76.779	−1676.342	−1550.226
600	112.545	119.345	−1675.300	−1487.319
800	120.135	152.873	−1673.498	−1424.931
1,000	124.771	180.210	−1693.394	−1361.437
1,200	128.252	203.277	−1691.366	−1295.228
1,400	131.081	223.267	−1686.128	−1229.393
1,600	133.361	240.925	−1686.128	−1163.934
1,800	135.143	256.740	−1683.082	−1098.841
2,000	136.608	271.056	−1679.858	−1034.096
2,200	138.030	284.143	−1676.485	−969.681
2,327	138.934	291.914	Melting temperature	
2,400	139.453	296.214	−1672.963	−905.582
2,600	140.959	307.435	−1669.279	−841.781
2,800	142.591	317.980	−2253.212	−776.335
3,000	144.474	327.841	−2244.729	−671.139

From [28]

Masimo Ex. 1042
IPR Petition - USP 10,627,783

6.3 Vaporization of Alumina

There is a detailed discussion of the vaporization behavior of alumina and other oxides in [29]. The main vapor species over alumina are Al, AlO, Al_2O, and AlO_2, depending on the temperature and oxidizing or reducing conditions in the surrounding atmosphere. Under reducing conditions Al and Al_2O are predominant; in 0.2 bar O_2, both AlO and AlO_2 are the main species [30].

Two examples of quantitative data of vapor pressure as a function of temperature are given in Table 15.

The boiling temperature of alumina at one atm pressure is about 3,530°C with a heat of vaporization of about 1,900 kJ mol^{-1} at 25°C [2], when compared with the melting temperature of 2,054°C, and a heat of fusion of about 109 kJ mol^{-1} at 25°C [31].

6.4 Thermal Conductivity

The thermal conductivity of α-alumina single crystals as a function of temperature is given in Table 16 (from [2, 23]). Heat is conducted through a nonmetallic solid by lattice vibrations or phonons. The mean free path of the phonons determines the thermal conductivity and depends on the temperature, phonon–phonon interactions, and scattering from lattice defects in the solid. At temperatures below the low temperature maximum (below about 40°K), the mean free path is mainly determined by the sample size because of phonon scattering from the sample surfaces. Above the maximum, the

Table 15 The pressure of AlO vapor and total vapor pressure in equilibrium with α-Al_2O_3 as a function of temperature, for reducing and neutral conditions

Temp. (K)	Log vapor pressure of AlO, *P* (bar) [29]
1,520	−15
1,630	−13
1,750	−11
1,900	−9
2,020	−7
2,290	−5
Temp. (K)	**Log total vapor pressure, *P* (atm.) [2, 31]**
2,309	−5.06
2,325	−4.99
2,370	−4.78
2,393	−4.77
2,399	−4.66
2,459	−4.42
2,478	−4.24
2,487	−4.04
2,545	−3.70
2,565	−3.89
2,605	−3.72

Masimo Ex. 1042
IPR Petition - USP 10,627,783

Table 16 Thermal conductivity of single crystal α-Al_2O_3

Temp. (K)	Conductivity ($J\ s^{-1}\ mK^{-1}$)	Temp. (°C)	Conductivity ($J\ s^{-1}\ mK^{-1}$)
0	0	25	36
10	1,200	100	29
20	3,800	300	16
40	5,900	500	10
50	5,000	700	7.5
60	2,300	900	6.3
80	790	1,100	5.9
100	400	1,300	5.9
200	100	1,500	5.4
		1,700	5.9
		1,900	6.3

From [2, 23]

conductivity decays approximately exponentially because of phonon–phonon inte tions. At high temperatures (above about 800°C), the phonon mean free path is of order of a lattice distance, and becomes constant with temperature. There is a m more detailed discussion of phonon behavior in ceramics and glasses in [23, 32]. ' velocity v of a phonon or sound wave in a solid can be found from the formula

$$v^2 = E/\rho \qquad ($$

in which E is Young's modulus and ρ is the density, so this velocity in alumin $10.1(10)^3\,m\ s^{-1}$ at 25°C. This result is close to the measured value of $10.845\,m\ s^{-1}$.

7 Electrical Properties

7.1 Electrical Conductivity

There have been a large number of studies of electrical conductivity of alumina, w widely different values being reported. Papers before 1961 are listed in [33] and thc from 1961 to 1992 in [34].

Anyone interested in the electrical conductivity of alumina should read carefu the papers of Will et al. [34]. These authors measured the electrical conductivity highly pure and dry sapphire from 400°C to 1,300°C; the elemental analysis of th sapphire samples is given in Table 17, and showed less than 35 ppm total impuritie Particularly significant is the low level of alkali metal impurities, which often provi ionic conduction in oxides.

The measurements in [34] were made with niobium foil electrodes with a guard ri configuration on disc samples, and in a vacuum of 10^{-7}–10^{-8} Torr. A nonsteady-sta voltage sweep technique was used for the measurements. The results are in Table 18 a Fig. 3 for conductivity along the x-axis. Between 700°C and 1,300°C, the activatic energy was about $460\,kJ\ mol^{-1}$ (4.8 eV) and between 400 and 700°C it was 39 kJ mol (0.4 eV). The great care taken with these measurements and the high purity of t sapphire make them definitive for the electrical conductivity for pure, dry alumina.

Masimo Ex. 1042
IPR Petition - USP 10,627,783

Table 17 Chemical analysis of sapphire for electrical conductivity measurements, from [34]

Element	Conc. (ppm)	Element	Conc. (ppm)
Iron	8	Potassium	<5
Silicon	6	Sodium	<3
Calcium	3	Nickel	<3
Magnesium	0.6	Chromium	<3
Beryllium	0.1	Lithium	<2

Table 18 Electrical conductivity of pure, dry sapphire

Temp. (°C)	Log conductivity ($ohm^{-1} cm^{-1}$)
1,300	7.46
1,200	8.48
1,100	9.70
1,000	11.14
900	12.88
800	14.24
700	15.20
600	15.32
500	15.70
400	16.08

From [34]

After 650 h electrolysis at 1,200°C, the conductivity remained constant, showing it was electronic and nonionic [34]. The authors [34] interpreted their results in terms of electrical conductivity of a wide-band semiconductor. The high-temperature portion resulted from intrinsic conductivity with equal numbers of holes and electrons as carriers; twice the activation energy gives the band gap of about 920 kJ mol^{-1}, or 9.6 eV, which is close to the band gap of 8.8 eV calculated from the optical absorption edge in the ultra-violet spectral range (see Sect. 9.2 on optical absorption). The low activation energy portion at low temperatures was attributed to extrinsic electronic conductivity from ionization of impurities. The authors suggested that silicon as a donor atom was the most likely impurity resulting in the low temperature conductivity. The interpretation of extrinsic conduction in the low activation range agrees well with the results of several other studies of the electrical conductivity of alumina [35–38], which showed close to the same conductivity and activation energy at high temperatures, but a transition to the low activation energy regime at higher temperatures than 700°C, presumably because of more impurities in the samples in those studies.

The electrical conductivity of alumina parallel to the *c*-axis was found to be a factor of 3.3 higher than perpendicular to this axis [34].

Of special interest are some experimental results for the conductivity at temperatures from about 1,800°C to near the melting temperature of 2,054°C of alumina [39], which fall very close to an extrapolation of the data from [34] up to 1,300°C, with the same activation energy. Thus the intrinsic electrical conductivity σ in/ohm cm from 700°C to the melting point follows the equation:

$$\log \sigma = 7.92 - 24{,}200 / T \qquad (9)$$

where T is in Kelvin.

Masimo Ex. 1042
IPR Petition - USP 10,627,783

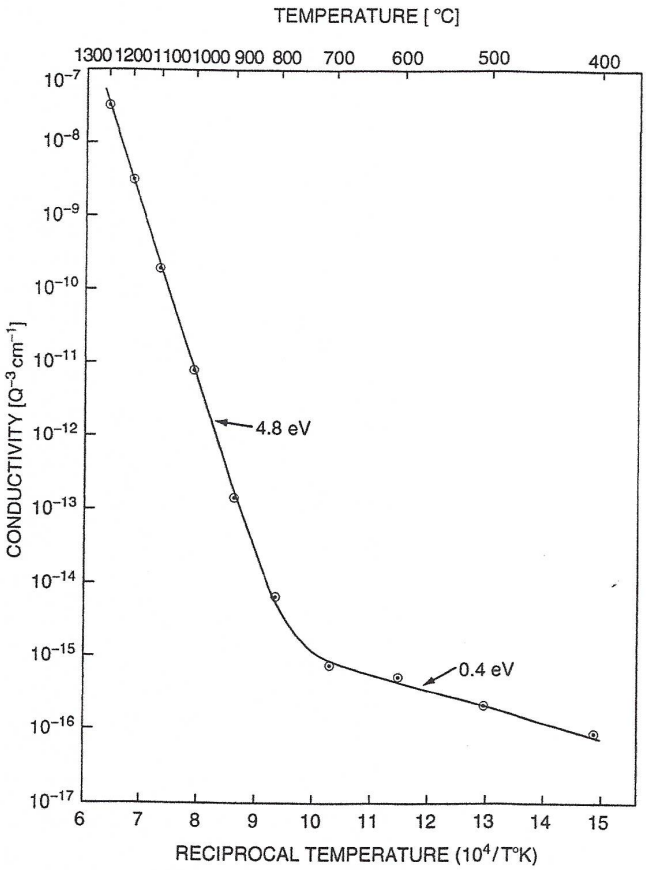


Fig. 3 The electrical conductivity of pure, dry sapphire along the *c*-axis. Points, measured values. From [34]

The electrolysis experiments of Ramirez et al. [40] show that when alumina contains some water (OH groups), the electrical conductivity results from the transport of hydrogen ions (actually hydronium ions, H_3O^+; see [41] for discussion).

The diffusion coefficient of H_3O^+ ions at 1,300°C calculated [41] from the experiments in [40] is $2.3(10)^{-9}\,cm^2s^{-1}$. This value is close to measured values of the diffusion coefficients of water in alumina [42]. Thus the mechanism of the diffusion of water in alumina is the transport of H_3O^+ ions, and these ions control the electrical conductivity when the water concentration is high enough.

To calculate the minimum concentration C of water in alumina that can contribute to the electrical conductivity, one can use the Einstein equation:

$$C = RT\sigma / Z^2F^2D \tag{10}$$

in which R is the gas constant, Z the ionic charge (valence), F the Faraday, and D the diffusion coefficient. The electrical conductivity at 1,300°C from [34] was 2.29

Masimo Ex. 1042
IPR Petition - USP 10,627,783

$\times 10^{-11}$/ohm cm. Thus with $D = 2.29(10)^{-9}\,cm^2\,s^{-1}$, a concentration of $1.13(10)^{-8}$ mol cm^{-3} of carriers results if one assumes that the conductivity in the samples in [34] results from H_3O^+ transport (which, of course, it does not); this concentration is $1.45(10)^{-7}$ carriers per Al atom in alumina. The concentration of H^+ in the alumina samples of [40] can be calculated from their highly sensitive infrared absorption measurements to be about $4.7(10)^{-7}$ per Al atom. Thus one can conclude that for H_3O^+ concentrations above about 10^{-8} mol cm^{-3} (3×10^{-7} ions per Al atom), there will be a contribution of these ions to the conductivity, whereas for lower H_3O^+ concentrations the conductivity will be mainly electronic.

The activation energy for water diffusion in alumina is about 220 kJ mol^{-1} (2.3 eV) from [42], so that many of the earlier results on electrical conductivity of alumina, for example, those summarized in [33], probably result from water transport at lower temperature; at higher temperatures, electronic conductivity will predominate, because of the high activation energy of intrinsic electronic conductivity. If the alumina is "dry" (H_3O^+ concentration below 10^{-8} mol cm^{-3}) low activation energy extrinsic electronic conduction will be dominant at lower temperatures, resulting from donor and receptor impurities in the alumina.

7.2 *Dielectric Properties*

The dielectric constant of alumina is given in Table 19 as a function of temperature and crystal orientation. The dielectric constant increases slightly up to 500°C, and is quite dependent on orientation. Very low dielectric loss values for sapphire have been reported [2], but are questionable. With reasonable purity, loss tangents below 0.001 are likely. Actual values probably depend strongly on crystal purity.

7.3 *Magnetic Properties*

Alumina is diamagnetic with a susceptibility less than 10^{-6} [2].

8 Diffusion in Alumina

Experimental volume diffusion coefficients of substances in alumina are summarized in ref. 41. Values for the parameters D_0 and Q (activation energy) from the Arrhenius equation:

$$D = D_0 \exp(-Q / RT) \tag{11}$$

Table 19 Dielectric constant of sapphire as a function of temperature at frequencies from 10^3 to 10^9 Hz (from [2]). Orientation to *c* axis

Temp. (°C)	I	II
25	9.3	11.5
300	9.6	12.1
500	9.9	12.5

Masimo Ex. 1042
IPR Petition - USP 10,627,783

The fastest diffusing substance in alumina is hydrogen (H_2). Fast-diffusing cation sodium, copper, silver, with hydroniums (H_3O^+) the fastest of these monovalent ons. Many other di- and trivalent cations have diffusion coefficients interme between these fast-diffusing ions and the slowest diffusers, the lattice elements al num and oxygen, which have about the same diffusion coefficients.

A number of experimenters have calculated diffusion coefficients D from "tail diffusion profiles in alumina, and attributed these D values to diffusion along dislocat subboundaries, or grain boundaries. However, this attribution is doubtful in most c as discussed in [41]. In only two studies [43, 44] is it likely true diffusion along g boundaries or dislocations was measured [41]. Mechanisms of diffusion in alu are uncertain; a variety of charged defects have been suggested to control diffusic alumina, but no interpretation is widely accepted because of discrepancies experimental results. I have suggested that oxygen and aluminum diffusion in alur results from transport of aluminum monoxide (AlO), and that AlO defects in alumina structure are important in diffusion. These speculations have some support, need more work to confirm them.

9 Chemical Properties

The decomposition of alumina at high temperatures can be deduced from its va pressure; see Sect. 6.3 and Table 15.

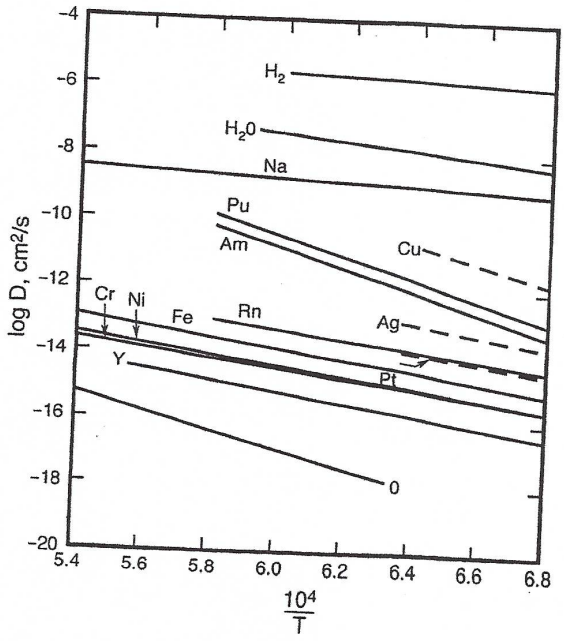


Fig. 4 Log diffusion coefficients vs. $10^4/T$ for selected substances diffusing in alumina. From [41

Masimo Ex. 1042
IPR Petition - USP 10,627,783

9.1 Reactions with Metals

The chemical reactions of alumina with other substances can best be explored from the thermodynamic properties of these reactions. If the Gibbs free energy ΔG of the reaction at a particular temperature is negative, the reaction tends to take place, and if ΔG this energy is positive the reaction tends not to occur. These considerations are modified by concentrations (more properly, thermodynamic activities) of the components as expressed in an equilibrium constant of the reaction. See books on thermodynamics for more details, for example [45].

The relative Gibbs free energies of the reactions of metals with oxygen tell whether or not a particular metal will displace the aluminum in alumina. The reaction of aluminum with oxygen is

$$\frac{4}{3}\mathrm{Al} + \mathrm{O_2} = \frac{2}{3}\mathrm{Al_2O_3} \tag{12}$$

All of the oxidation reactions with metals are written with one mole of O_2 reacting for consistent comparison. This is the format for reactions plotted in an Ellingham diagram (see [46]). The Gibbs free energies of some of these oxidation reactions are given in Table 20, taken from [28, 29, 46–48]. If the Gibbs free energy of the reaction is higher than that of aluminum ($-845.6\,\mathrm{kJ\ mol^{-1}}$ for reaction (12)), then this metal will react with alumina, displacing all the aluminum in any alumina in contact with the metal, either solid, liquid, or vapor. For example for yttrium:

$$\frac{4}{3}\mathrm{Y} + \mathrm{O_2} = \frac{2}{3}\mathrm{Y_2O_3} \tag{13}$$

the Gibbs free energy is $-1017\,\mathrm{kJ\ mol^{-1}}$, so yttrium will displace aluminum from alumina:

$$2\mathrm{Y} + \mathrm{Al_2O_3} = 2\mathrm{Al} + \mathrm{Y_2O_3} \tag{14}$$

The free energy change of reaction 14 can be deduced from the values for Eqs. (12) and (13) from Table 20 to be $-256\,\mathrm{kJ\ mol^{-1}}$, showing the tendency for yttrium to displace aluminum. If the free energy shown in Table 20 is less than that for oxidation of aluminum, the metal will not react with alumina. Thus at 1,000°C, sodium and potassium vapors (1 atm) do not react with alumina, but 1 atm. of lithium vapor does. Liquid alkaline earths metals such as Mg, Ca, Sr, and Ba react with alumina at 1,000°C and displace aluminum metal. The relative tendency of reactions of solid and liquid metals with alumina does not change much with temperature. Of course at low temperatures (below about 500°C), the rates of reactions can be slow, even if the thermodynamics show a tendency to react. Gibbs free energies for other temperatures can be calculated from data in the thermodynamic tables in [28, 29, 46–48].

9.2 Reactions with Nonmetals

The halides Cl_2, Br_2, and I_2 do not react with alumina, but fluorine (F_2) does:

$$2\mathrm{Al_2O_3} + 6\mathrm{F_2} = 4\mathrm{AlF_3} + 3\mathrm{O_2} \tag{15}$$

Masimo Ex. 1042
IPR Petition - USP 10,627,783

Table 20 Gibbs Free energies of reactions of metals with 1 atm. of oxygen at 1,000°C from [28, 29, 46–48]

Solid metals	$-\Delta G$ (kJ mol^{-1})	Liquid metals	$-\Delta G$
Y	1,017		
Zr	849	Ca	1,013
Ti	678	CE	962
Si	644	Mg	937
V	619	Ba	879
Mn	586	Li	870
Cr	544	Al	845.6
One atm. of metal vapor	$-\Delta G$ (kJ/mol)		
Na	444		
Zn	418		
K	326		

Metal + O_2 = oxide

At 1,000°C the Gibbs free energy for this reaction is about −2133 kJ mol^{-1}, showing a strong tendency to react.

Reactions of the gases H_2, H_2O, CO, and CO_2 with alumina can be deduced from the reactions:

$$Al_2O_3 + 3H_2 = 2Al + 3H_2O \quad (16)$$

$$Al_2O_3 + 3CO = 2Al + 3CO_2 \quad (17)$$

At equilibrium at 1,000°C the ratio of H_2/H_2O is about 10^{10} and CO/CO_2 about $2(10)^{10}$. It is impossible to reduce the water or carbon dioxide levels so low in any practical reaction process, so effectively H_2 and CO do not reduce Al_2O_3. Even at 2,000°C these ratios are about $3(10)^4$ and $2(10)^5$, which are difficult levels to maintain in practice. A possible reaction of alumina with carbon is

$$2Al_2O_3 + 6C = Al_4C_3 + 3CO_2 \quad (18)$$

However, the Gibbs free energy of this reaction is +1131 kJ mol^{-1} at 1,000°C and +504.6 kJ mol^{-1} at 2,000°C, so it will take place only at very low carbon dioxide concentrations.

Other chemical reactions of alumina can be examined with the thermodynamic data in [28–30, 47–48].

9.3 *Reactions of Alumina in Aqueous Solutions*

Alumina is amphoteric, which means that it dissolves in acidic and basic solutions, but not in neutral aqueous solutions. The solubility of alumina in solutions of pH from about 4–9 is low; at 25°C it is less than 10^{-7} mol l^{-1} at pH 6 [1]. Alternatively, alumina dissolves readily in strong acids (HCl, HNO_3, H_2SO_4) and strong bases (NaOH, KOH) at temperatures well above ambient (e.g., 90°C).

Masimo Ex. 1042
IPR Petition - USP 10,627,783

10 Optical Properties

10.1 Refractive Index

The optical properties of solids can be studied with the complex refractive index n^*:

$$n^* = n + ik \tag{19}$$

in which n is the real part of the refractive index and k is the imaginary part or absorption index. Values of n and k from 0.008731 μm to 600 μm (142.000–0.00207 eV) are given to high accuracy and many wavelengths for alumina in [49]. In the wavelength range from 0.1454 μm to 4.000 μm (8.529–0.31 eV), the value of k for highly pure alumina is less than 10^{-6} [49, 50], so the alumina is effectively transparent. Values of n for this wavelength range are given to four significant figures in Table 21. Values of n in the fifth or sixth significant figure are different for different investigations, probably because of different purities of samples and different measuring techniques and errors. A two-term equation for n (ordinary ray) in this wavelength range is [2]

$$n = 1.74453 + \frac{0.0101}{\lambda - 0.1598} \tag{20}$$

with λ the wavelength in micrometers. This equation gives n accurately to about four significant figures (Table 21). A more accurate three-term Sellmeier equation is

$$n^2 - 1 = \frac{A_1 \lambda^2}{\lambda^2 - \lambda_1^2} + \frac{A_2 \lambda^2}{\lambda^2 - \lambda_2^2} + \frac{A_3 \lambda^2}{\lambda^2 - \lambda_3^2} \tag{21}$$

with the constants A_i and λ_i given in Table 22.

10.2 Optical Absorption

The absorption limit of 8.73 eV in Table 23 is close to the band gap of 8.8 eV for alumina. At energies lower than 8.73 eV, trace impurities and defects in the alumina lead to absorption tails as described in [49]. Values of n and k at higher energies than 8.73 eV are given in Table 23 to three or four significant figures. Values from different research groups can vary substantially [49]; those in Table 23 are from [50]. See [49] for n and k values at many more energies (wavelengths).

The values of k in Table 23 show a maximum at about 13 eV, which can be attributed to exitonic absorption [49]; other electronic processes in the ultra-violet spectral range are also described in [49].

Appreciable absorption begins in the infrared spectral range above a wavelength of 4.0 μm, as shown in Table 24; there are absorption peaks at 17.24 μm (580 cm^{-1}) and 22.73 μm (440 cm^{-1}), which result from lattice vibrations. For more details see [49].

The optical anisotropy of alumina results in slightly different n and k values for the ordinary and extraordinary ray, as shown in detail in [49] (see Table 22). This anisotropy is related to the hexagonal (rhombohedral) structure of the alumina.

Masimo Ex. 1042
IPR Petition - USP 10,627,783

Table 21 Refractive Index of sapphire at 25°C in the spectral range where $k < 10^{-6}$, from

Wavelength, λ, (μm)	Refractive index, n	Wavelength, λ (μm)	Refractive
0.1464	2.231	1.367	1.749
0.1603	2.070	1.530	1.747
0.1802	1.947	1.709	1.743
0.200	1.913	1.960	1.738
0.220	1.878	2.153	1.734
0.240	1.854	2.325	1.731
0.260	1.838	3.244	1.704
0.280	1.824	3.507	1.695
0.300	1.815	3.707	1.687
0.330	1.804	4.000	1.675
0.361	1.794		
0.405	1.786		
0.436	1.781		
0.486	1.775		
0.546	1.771		
0.579	1.769		
0.644	1.765		
0.707	1.763		
0.852	1.759		
0.894	1.758		
1.014	1.755		

Table 22 Refractive index [16], constants at 20°C from 0.2 to 5.5 mm, from [49, 50]

Term	Ordinary ray	Extraordinary ray
λ_1	0.0726631	0.0740298
λ_2	0.1193242	0.1216529
λ_3	18.028251	20.072248
A_1	1.4313493	1.5039759
A_2	0.65054713	0.5506141
A_3	5.3414021	6.5927379

The refractive index of alumina increases slightly with increasing temperature the visible and near-visible spectral range. The value of the temperature coefficien dT of the refractive index from wavelengths 0.4–0.8 μm is about $13(10)^{-6}°K^{-1}$ [49

10.3 Color of Alumina

Without impurities alumina is colorless. However, addition of transition metal ion alumina leads to spectacular colors, gem stones, and practical applications such ruby lasers. Many aspects of color are discussed in detail in [51].

With the addition of about 1% of Cr_2O_3 to Al_2O_3 (replacement of one out of hundred of the aluminum ions with chromium ions), alumina acquires a beautiful color and is known as ruby, one of the most prized gem stones. The red color res from transitions of electrons between energy levels in the ruby, as described in [5 p. 8Iff. Ruby also shows a bright red fluorescence when it is illuminated with ul violet light (energy of 4–5 eV). Ruby also shows pleochoism (multicolors); in pol ized light the color changes as the ruby crystal is rotated [51].

Masimo Ex. 1042
IPR Petition - USP 10,627,783

Table 23 Refractive index, n, and absorption index, k, of the ordinary ray for sapphire in the ultra-violet spectral range, at 25°C, from [49, 50]

Energy (eV)	Wavelength, λ, (μm)	n	k
142.000	0.008731	0.975	0.0130
120.000	0.010330	0.972	0.0177
100.206	0.01237	0.892	0.088
79.996	0.01550	0.929	0.130
60.001	0.02066	0.911	0.136
42.000	0.02952	0.859	0.098
30	0.04133	0.841	0.367
27.013	0.04590	0.605	0.317
24.113	0.05142	0.524	0.542
19.992	0.06202	0.800	0.983
18.008	0.06885	1.028	1.093
15.475	0.08012	1.142	1.125
13.582	0.09129	1.375	1.434
12.972	0.09558	2.581	1.573
12.361	0.1003	1.981	1.476
11.263	0.1101	2.400	1.131
10.292	0.1205	2.441	0.831
9.523	0.1302	2.559	0.686
8.852	0.1401	2.912	0.125
8.791	0.1410	2.841	0.037
8.760	0.1415	2.797	0.011
8.730	0.1420	2.753	0

Table 24 Refractive index, n, and absorption index, k, of the ordinary ray for sapphire in the infrared spectral range, at 25°C, from [49]

Wavelength, λ, (μm)	n	k
4.000	1.675	$1.30\ (10)^{-6}$
5.000	1.624	$3.76\ (10)^{-5}$
7.143	1.459	$3.60\ (10)^{-3}$
10.00	0.88	0.053
10.99	0.27	0.224
12.05	0.08	1.04
12.99	0.07	1.57
14.93	0.10	2.96
16.13	0.47	3.56
16.95	0.75	6.30
17.24	1.69	11.28
17.86	9.10	1.53
19.23	3.82	0.115
20.00	2.64	0.106
22.73	10.08	14.01
25.00	4.64	0.156
30.30	3.95	0.0145
33.33	3.69	0.00668
50.00	3.26	0.0117
60.13	3.19	0.0130
82.71	3.13	0.0085
100.0	3.12	0.0070
200.0	3.08	0.0035
333.3	3.07	0.0027
600.0	3.05	0.0015

Masimo Ex. 1042
IPR Petition - USP 10,627,783

The deep blue color or sapphire gems results from the addition of a few hundredths of one percent of iron and titanium impurities to alumina. The Fe^{2+} and Ti^{4+} ions substitute for aluminum in the sapphire, and when light of energy of 2.11 eV is shone on the sapphire, it is absorbed by the charge transfer reaction:

$$Fe^{2+} + Ti^{4+} = Fe^{3+} + Ti^{3+} \quad (22)$$

See [51], p. 140ff for a complete description of this process.

A variety of other colors are found in natural and synthetic alumina crystals [2, 51]. For example, an orange-brown color is produced by Cr^{4+} (padparadscha sapphire) [51]; different transition metal ions in different concentrations and oxidation states produce many colors.

11 Conclusion and Future Uses of Alumina

The properties of alumina listed in Sects. 4–10 show the unusual performance of pure alumina, leading to the variety of applications given in Table 1. Practical aluminas with impurities and defects have somewhat degraded properties, but often are superior to many other materials, and have a variety of specialized applications such as refractories, electronic components, and catalyst substrates. In [1] there are articles discussing the future of alumina. There will continue to be incremental improvements in processing methods and properties, leading to expansion of present applications. What really new areas of application of alumina are likely? These predictions are speculative, but the most promising new applications of alumina will probably be in electronic circuits, optical components, and biomaterials. Alumina fibers for composites and optics are attractive if they can be made pure, defect-free, and cheap. Because of its excellent properties other unsuspected applications of alumina will undoubtedly be developed.

Reference

1. L.D. Hart (ed.), *Alumina Chemicals*, The American Ceramic Society, Westerville, OH, 1990.
2. W.H. Gitzen, *Alumina as a Ceramic Material*, The American Ceramic Society, Westerville, OH, 1970.
3. Emphasizes defects and interfaces, especially grain boundaries, in alumina, *J. Am. Ceram. Soc.* **77**, [2] (1994).
4. Emphasizes grain boundaries, grain growth, and diffusion in alumina, *J. Am. Ceram. Soc.* **86** [4] (2003).
5. P. Richet, J.A. Xu, and H.K. Mao, Quasi-hydrostatic compression of ruby to 500 kbar, Phys. Chem. Min. **16**, 207–211 (1988).
6. A.P. Jephcoat, R.J. Hemley, H.K. Mao, and K.A. Goettel, X-ray diffraction of ruby (Al_2O_3: Cr^{3+}) to 175 GPa, *Physica B* **150**, 115–121 (1988).
7. K.T. Thomson, R.M. Wentzcovitch, and M.S.T. Bukowinski, Polymorphs of alumina predicted by first principles, *Science* **274**, 1880–1882 (1996).
8. A.H. Carim, G.S. Rohrer, N.R. Dando, S.Y. Tzeng, C.L. Rohrer, and A.J. Perrotta, Conversion of diaspore to corundum, *J. Am. Ceram. Soc.* **80**, 2677–80 (1997).
9. R.L. Coble, Transparent Alumina and Method of Preparation, U.S. Patent 3,026,210, March 20 (1967).

Masimo Ex. 1042
IPR Petition - USP 10,627,783

10. F.J. Klug, S. Prochazka, and R.H. Doremus, Alumina-silica phase diagram in the mullite region, *J. Am. Ceram. Soc.* **70**, 750–759 (1987).
11. E.N. Bunting, Phase equilibrium in the system Cr3O3–Al2O3, *Bur. Stand. J. Res.* **6**, 947–949 (1931).
12. E.M. Levin, C.R. Robbins, and H.F. *McMurdie, Phase Diagrams for Ceramists*, Vol. I–XIII, The American Ceramic Society, 1964–2002.
13. D.M. Roy and R.E. Barks, Subsolidus phase equilibrium in Al2O3–Cr2O3, *Nature*, **235**, 118–119 (1972).
14. C. Greskovich and J.A. Brewer, Solubility of magnesia in polycrystalline alumina at high temperatures, *J. Am. Ceram. Soc.* **84**, 420–425 (2001).
15. J.H. Gieske and G.R. Barsch, Pressure dependence of the elastic constants of single crystalline aluminum oxide, *Phys. Status Solidi* **29**, 121–131 (1967).
16. A. Kelly, *Strong Solids*, Chap. 1, Oxford University Press, London, 1973.
17. S.M. Wiederhorn in Mechanical and Thermal Properties of Ceramics, J.B. Wachtman, (ed.), NBS Special Publications 303, U.S. GPO, Washington, D.C., 1969, p. 217.
18. R.H. Doremus, Cracks and energy-criteria for brittle fracture, *J. Appl. Phys.* **47**, 1833–1836 (1976).
19. R.H. Doremus, Fracture statistics: A comparison of the normal, Weibull and type I extreme value distributions, *J. Appl. Phys.* **54**, 193–201 (1983).
20. S.C. Carniglia, Reexamination of experimental strength – vs. – grain – size data for ceramics, *J. Am. Ceram. Soc.* **55**, 243 (1972).
21. J.E. Burke, R.H. Doremus, W.B. Hillig, and A.M. Turkalo, Static Fatigue in Glasses and Alumina, in Materials Sci. Res. Vol. 5, W.W. Kriegel (ed.), Plenum Press, New York, 1971, pp. 435–444.
22. N.W. Thibault and H.Z. Nyquist, The measured Knoop hardness of hard substances and factors affecting its determination, *Trans. Am. Soc. Metals* **38**, 271–330 (1947).
23. W.D. Kingery, H.K. Bowen, and D.R. Uhlmann, *Introduction to Ceramics*, Wiley, New York (1976).
24. W.R. Cannon and T.G. Langdon, Creep of Ceramics, *J. Mater. Sci.* **18**, 1–50 (1983); **23**, 1–20 (1988).
25. A.H. Hynes and R.H. Doremus, Theories of creep in ceramics, *Crit. Rev. Solid State Mater. Sci.* **21**, 1–59 (1996).
26. M.L. Kronberg, Plastic deformation of single crystals of sapphire: Basal slip and twinning, *Aeta Met.* **5**, 507–529 (1957).
27. J.D. Snow and A.H. Heuer, Slip systems in Al2O3, *J. Am. Ceram. Soc.* **56**, 153–157 (1973).
28. M.W. Chase, NIST – JAVAF Thermochemical Tables, *J. Phys. Chem. Ref. Data, Monograph* **9**.
29. R.H. Tamoreaux, D.L. Hildenbrand and L. Brewer, High temperature vaporization behavior of oxides, *J. Phys. Chem. Ref. Data* **16**, 412 (1987).
30. L. Brewer and A.W. Searcy, Gaseous species of the Al–Al_2O_3 system, *J. Am. Chem. Soc.* **73**, 5308–5314 (1951).
31. R.V. Gains, H.C.W. Skinner, E.E. Foord, B. Mason, and A. Rosenzweig, *Dana's New Mineralogy*, Wiley, New York, 1977, p. 214.
32. E. Schreiber and O.L. Anderson, Pressure derivatives of the sound velocities of polycrystalline alumina, *J. Am. Ceram. Soc.* **49**, 184–190 (1966).
33. J. Pappis and W.D. Kingery, Electrical properties of single and polycrystalline alumina at high temperatures, *J. Am. Ceram. Soc.* **44**, 459 (1961).
34. F.G. Will, H.G. Lorenzi, and K.H. Janora, *J. Am. Ceram. Soc.* **75**, 295–304, 2790–2791 (1992).
35. O.T. Özkan and A.J. Moulson, The electrical conductivity of single crystal and polycrystalline aluminum oxide, *British J. Appl. Phys.* **3**, 983 (1970).
36. H.P.R. Frederike and W.R. Hosler, High temperature electrical conductivity of aluminum oxide, *Mater. Sci. Res.* **9**, 233 (1973).
37. K. Kituzawa and R.L. Coble, Electrical conduction in single crystal and polycrystalline Al2O3 at high temperature, *J. Am. Ceram. Soc.* **57**, 245 (1979).
38. H.M. Kizilyalli and P.R. Mason, DC and AC electrical conduction in single crystal alumina, *Phys. Status Solidi* **36**, 499 (1976).
39. E.E. Shpilrain, D.N. Kagan, L.S. Barkhatov, and L.I. Zhmakin, The electrical conductivity of alumina near the melting point, High Temperatures – High Pressures **8**, 177 (1976).
40. R. Ramirez, R. Gonzalez, J. Colera, and Y. Chen, Electric-field-enhanced diffusion of deuterons and protons in α-Al2O3 crystals, *Phys. Rev. B* **55**, 237–242 (1997).
41. R.H. Doremus, Diffusion in Alumina, *J. Appl. Phys.* **101**, 101301 (2006).

Masimo Ex. 1042
IPR Petition - USP 10,627,783

42. J.D. Fowler, D. Chandra, T.S. Elleman, A.W. Payne, and K. Verghese, Tritium diffusic and BeO, *J. Am. Ceram. Soc.* **60**, 55 (1977).
43. V.S. Stubican and J.W. Orenbach, Influence of anisotropy and doping on grain-bounda in oxide systems, *Solid State Ionics* **12**, 375 (1984).
44. X. Tang, and K.P.D. Lagerof, and A.H. Heuer, Determination of pipe diffusion coe undoped and magnesia doped sapphire (α-Al2O3); a study based on annihilation of dipoles, *J. Am. Ceram. Soc.* **86**, 560–565 (2003).
45. D.R. Gaskell, *Introduction to the Thermodynamics of Materials*, 4th edn.,Taylor a New York, 2003.
46. L.S. Darken and N.W. Gurry, *Physical Chemistry of Metals*, McGraw-Hill, New York
47. A. Paul, *Chemistry of Glasses*, Chapman and Hall, London, 1982, p. 157.
48. R.H. Doremus, *Diffusion of Reactive Molecules in Solids and Melts*, Wiley, New York 71, 191.
49. M.E. Thomas and W.J. Tropf in *Handbook of Optical Constants of Solids III*, E (ed.), Academic Press, New York, 1998, p. 653.
50. L.H. Malitson and M.J. Dodge, Refractive index and birefringence of synthetic sapphi *Soc. Am.* **62**, 1405 (1972).
51. K. Nassau, *The Physics and Chemistry of Color*, Wiley, New York, 1983.

Masimo Ex. 1042
IPR Petition - USP 10,627,783